Chapter 5
Energy Harvesting for Wireless Relaying Systems

Yunfei Chen

5.1 Introduction

In wireless communications, the destination node may be too far away from the source node, or it may be obstructed from the source node, such that direct communications between them are not possible. In this case, idle nodes between them can be used to form a relaying link [1, 2]. Even when direct communications between source and destination are available, idle nodes can still be used to provide extra links. Thus, in wireless relaying, the relaying nodes forward signals from the source to the destination to extend network coverage or to achieve diversity gain.

However, one of the main problems of existing wireless relaying systems is that the relaying node has to consume its own energy to perform the relaying operation. This discourages idle nodes from taking part in relaying, especially when they operate on batteries and hence have a limited lifetime. Energy harvesting can solve this problem by allowing the relaying node to harvest wireless energy from the source and to use the harvested energy for relaying. Thus, this chapter investigates energy harvesting wireless relaying. Figure 5.1 compares the conventional wireless relaying with energy harvesting relaying. One sees that their main difference is that energy harvesting relaying has an extra energy link between source and relay so that the source can transfer energy to the relay wirelessly.

There are two main relaying protocols: amplify-and-forward (AF) and decode-and-forward (DF) [3, 4]. In AF, the signal from the source is amplified and then forwarded to the destination without any further processing. The amplification and forwarding operations will consume energy. In DF, the signal from the source

Y. Chen (✉)
University of Warwick, Coventry CV4 7AL, UK
e-mail: yunfei.chen@warwick.ac.uk

D.N.K. Jayakody et al. (eds.), *Wireless Information and Power Transfer: A New Paradigm for Green Communications*, DOI 10.1007/978-3-319-56669-6_5

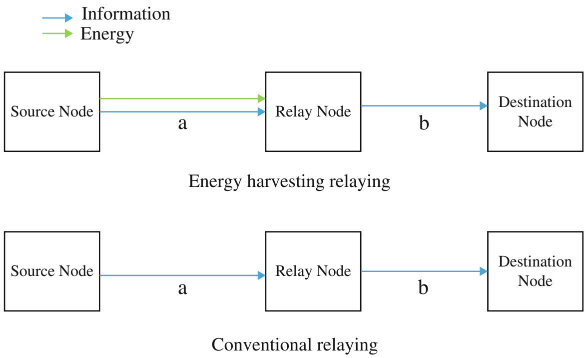

Fig. 5.1 Comparison of conventional and energy harvesting relaying

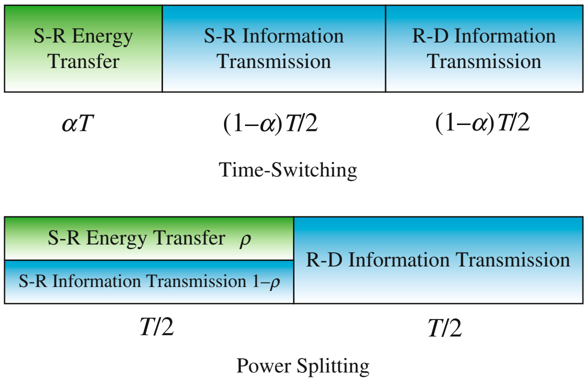

Fig. 5.2 TS and PS strategies for wireless relaying

is first decoded and then re-encoded before being forwarded to the destination. The decoding, encoding and forwarding operations will also consume energy. The AF protocol is simpler than the DF protocol by performing a straightforward amplification without any decoding but its performance is usually poorer than the DF protocol due to the amplified noise.

On the other hand, there are two main energy harvesting strategies: time-switching (TS) and power-splitting (PS) [5]. In TS, a dedicated harvesting time is allocated for energy harvesting. This simplifies the hardware requirement but the dedicated harvesting time reduces the throughput or achievable rate of the system. In PS, no dedicated harvesting time is allocated but a portion of the received power is split for energy harvesting. This strategy keeps the throughput of the system but increases the hardware requirement, as a power splitter is not trivial in the implementation. Figure 5.2 compares the TS and PS strategies. In this figure, T is the total transmission time in wireless relaying, α is the so-called TS coefficient that determines how much time will be dedicated for harvesting, and ρ is the so-called PS factor that determines how much of the received power should be split for harvesting.

In this chapter, we consider both TS and PS for AF and DF protocols. For simplicity, we only consider a three-node relaying system, where the signal is transmitted from the source to the relay and then forwarded to the destination, without a direct link between source and destination. Each node is also half-duplex and has a single antenna.

5.2 Energy Harvesting DF Relaying Without Interference

5.2.1 Introduction

In this section, we show the performance of energy harvesting DF relaying without interference. As mentioned before, DF normally offers better performance than AF and thus, it is preferred in applications that emphasize performances. On the other hand, compared with TS, the PS scheme does not require any dedicated harvesting time. Thus, PS normally has higher throughput. Considering these, in this section, the performance of DF using PS will be studied.

Several previous works on DF relaying using energy harvesting exist. For example, reference [6] used stochastic geometry theories to study the effect of random location on the outage probability of DF using PS. Reference [7] studied the approximate ergodic capacity of DF using both TS and PS. Reference [8] considered interference for DF relaying using TS. Reference [9] compared full-duplex and half-duplex DF relaying systems using TS. This was extended to the multiple antenna case in [10]. All of them assumed Rayleigh fading channels. There were no results on bit error rate (BER) either.

In this section, the exact BER and throughput performances of DF using PS will be studied for Nakagami-*m* fading channels. Two different transmission scenarios will be considered: instantaneous transmission with known channel state information and delay- or error-tolerant transmission with averaged error rate or throughput. For each scenario, exact analytical expressions for the end-to-end BER and throughput will be derived. These expressions will then be used to study the optimum PS factor, a key parameter for energy harvesting relaying. Design guidance on energy harvesting relaying will be provided based on the study.

As mentioned before, we consider a three-node DF relaying system using PS but without a direct link. From Fig. 5.2, the source transmits a signal to the relay in the first phase. The relay splits this signal into two parts: one part for energy harvesting and one part for information decoding. The decoded information is then encoded again and forwarded to the destination using the harvested energy. Thus, the part of the received signal at the relay for information decoding is

$$y_k^r = \sqrt{(1-\rho)P_S}hs + \sqrt{1-\rho}n_k^{\mathrm{ra}} + n_k^{\mathrm{rc}}. \tag{5.1}$$

In the above equation, P_S is the transmitted power of the source, ρ is the PS factor to be optimized, h is the Nakagami-m fading gain of the source-to-relay link, s is the transmitted binary phase shift keying (BPSK) bit such that $s = +1$ and $s = -1$

with equal probabilities, n_k^{ra} is the k-th sample of the noise from the antenna and n_k^{rc} is the k-th sample of the noise from the RF-to-baseband conversion, assumed to be additive white Gaussian noise (AWGN) with mean zero and variance σ_{ra}^2 and σ_{rc}^2, respectively, and the fading power $|h|^2$ is Gamma distributed with $f_{|h|^2}(x) = \left(\frac{m_1}{\Omega_1}\right)^{m_1} \frac{x^{m_1-1}}{\Gamma(m_1)} e^{-\frac{m_1}{\Omega_1}x}, x > 0$, m_1 is the Nakagami m parameter, Ω_1 is the average fading power of the source-to-relay link and $\Gamma(\cdot)$ is the complete Gamma function [11, Eq. (8.310.1)].

The other part of the received signal for energy harvesting can give the harvested energy $E_h = \eta\rho P_S|h|^2\frac{T}{2}$ so that the transmission power of the relay is $P_r = \frac{E_h}{T/2} = \eta\rho P_S|h|^2$, where η is the conversion efficiency of the energy harvester used. Using the harvested energy calculated, one has the received signal at the destination as

$$y_k^d = \sqrt{P_r} g\hat{s} + n_k^{\mathrm{da}} + n_k^{\mathrm{dc}} \tag{5.2}$$

where P_r is the transmission power of the relay given before, g is the Nakagami-m fading gain of the relay-to-destination link, $\hat{s}$ is the data decision of the BPSK bit made and transmitted by the relay, and n_k^{da} and n_k^{dc} are the antenna noise and the conversion noise, respectively. In this case, $|g|^2$ is Gamma distributed $f_{|g|^2}(x) = \left(\frac{m_2}{\Omega_2}\right)^{m_2} \frac{x^{m_2-1}}{\Gamma(m_2)} e^{-\frac{m_2}{\Omega_2}x}, x > 0$, where m_2 is the Nakagami m parameter and Ω_2 is the average fading power of the relay-to-destination link. Also, n_k^{da} and n_k^{dc} are AWGN with mean zero and variance σ_{da}^2 and σ_{dc}^2, respectively.

5.2.2 BER

Using (5.1) and (5.2), the BERs of the S-R and R-D links are derived as $\mathrm{BER}_r = \frac{1}{2}\mathrm{erfc}(\sqrt{\gamma_1})$ and $\mathrm{BER}_d = \frac{1}{2}\mathrm{erfc}(\sqrt{\gamma_2})$, respectively, where $\gamma_1 = \frac{(1-\rho)P_S|h|^2}{(1-\rho)\sigma_{\mathrm{ra}}^2+\sigma_{\mathrm{rc}}^2}$ is defined as the instantaneous signal-to-noise ratio (SNR) of the S-R link, $\gamma_2 = \frac{\eta\rho P_S|h|^2|g|^2}{\sigma_{\mathrm{da}}^2+\sigma_{\mathrm{dc}}^2}$ is defined as the instantaneous SNR of the R-D link, and $\mathrm{erfc}(\cdot)$ is the complementary error function [11, Eq. (8.250.4)].

For instantaneous transmission, h and g are known through channel estimation. Thus, the end-to-end BER of the whole relaying link can be derived as $\mathrm{BER} = \mathrm{BER}_r(1-\mathrm{BER}_d) + \mathrm{BER}_d(1-\mathrm{BER}_r)$ or

$$\begin{aligned}\mathrm{BER} = {} & \frac{1}{2}\mathrm{erfc}\left(\sqrt{\frac{(1-\rho)P_S|h|^2}{(1-\rho)\sigma_{\mathrm{ra}}^2+\sigma_{\mathrm{rc}}^2}}\right) + \frac{1}{2}\mathrm{erfc}\left(\sqrt{\frac{\eta\rho P_S|h|^2|g|^2}{\sigma_{\mathrm{da}}^2+\sigma_{\mathrm{dc}}^2}}\right) \\ & -\frac{1}{2}\mathrm{erfc}\left(\sqrt{\frac{(1-\rho)P_S|h|^2}{(1-\rho)\sigma_{\mathrm{ra}}^2+\sigma_{\mathrm{rc}}^2}}\right)\mathrm{erfc}\left(\sqrt{\frac{\eta\rho P_S|h|^2|g|^2}{\sigma_{\mathrm{da}}^2+\sigma_{\mathrm{dc}}^2}}\right).\end{aligned} \tag{5.3}$$

One sees that, when the hop SNRs are large, the third term in (5.3) is much smaller than the first two terms and may be ignored. In this case, when the value of ρ increases, the first term in (5.3) increases while the second term in (5.3) decreases. Thus, there exists an optimum value of ρ that minimizes the BER. This optimum value can be derived using standard mathematical manipulations of first-order differentiation but there is no closed-form expression for the optimum value of ρ.

For error-tolerant transmission, the average end-to-end BER can be calculated as

$$\bar{\text{BER}} = \int_0^\infty \int_0^\infty \left[\frac{1}{2}\text{erfc}\left(\sqrt{\frac{(1-\rho)P_S x}{(1-\rho)\sigma_{\text{ra}}^2 + \sigma_{\text{rc}}^2}}\right) + \frac{1}{2}\text{erfc}\left(\sqrt{\frac{\eta\rho P_S xy}{\sigma_{\text{da}}^2 + \sigma_{\text{dc}}^2}}\right) - \frac{1}{2}\text{erfc}\left(\sqrt{\frac{(1-\rho)P_S x}{(1-\rho)\sigma_{\text{ra}}^2 + \sigma_{\text{rc}}^2}}\right)\text{erfc}\left(\sqrt{\frac{\eta\rho P_S xy}{\sigma_{\text{da}}^2 + \sigma_{\text{dc}}^2}}\right)\right] f_{|h|^2}(x) f_{|g|^2}(y)\,dxdy. \tag{5.4}$$

5.2.3 Throughput

Similarly, the throughput of the S-R and R-D can be derived from the received signals as $C_r = \ln(1+\gamma_1)$ and $C_d = \ln(1+\gamma_2)$, respectively.

For instantaneous transmission, the fading channel gains are known. Using them, the end-to-end throughput of the DF relaying system can be derived as

$$C = \min\{C_r, C_d\} = \ln\left(1 + \min\left\{\frac{(1-\rho)P_S|h|^2}{(1-\rho)\sigma_{\text{ra}}^2 + \sigma_{\text{rc}}^2}, \frac{\eta\rho P_S|h|^2|g|^2}{\sigma_{\text{da}}^2 + \sigma_{\text{dc}}^2}\right\}\right). \tag{5.5}$$

This throughput also has an optimum value of ρ. The optimum value of ρ can be derived as $\rho_{\text{opt}}^C = \frac{(\sigma_{\text{da}}^2+\sigma_{\text{dc}}^2+\eta|g|^2\sigma_{\text{rc}}^2+\eta|g|^2\sigma_{\text{ra}}^2)-\sqrt{\Delta}}{2\eta|g|^2\sigma_{\text{ra}}^2}$, where $\Delta = [\eta|g|^2\sigma_{\text{rc}}^2]^2 + 2(\eta|g|^2\sigma_{\text{rc}}^2)(\sigma_{\text{da}}^2+\sigma_{\text{dc}}^2+\eta|g|^2\sigma_{\text{ra}}^2)+(\sigma_{\text{da}}^2+\sigma_{\text{dc}}^2-\eta|g|^2\sigma_{\text{ra}}^2)^2$. One sees that this optimum ρ does not depend on $|h|^2$. As well, when $\frac{|g|^2}{\sigma_{\text{da}}^2+\sigma_{\text{dc}}^2}$ is large and goes to infinity, ρ_{opt}^C approaches zero.

For delay-tolerant transmission, the ergodic throughput is obtained by averaging it over the channel gains such that only the channel statistics are needed. Using this, the ergodic capacity can be calculated as

$$\bar{C} = \int_0^\infty \int_0^\infty \ln\left(1 + \min\left\{\frac{(1-\rho)P_S x}{(1-\rho)\sigma_{\text{ra}}^2 + \sigma_{\text{rc}}^2}, \frac{\eta\rho P_S xy}{\sigma_{\text{da}}^2 + \sigma_{\text{dc}}^2}\right\}\right) f_{|h|^2}(x) f_{|g|^2}(y)\,dxdy. \tag{5.6}$$

The ergodic throughput in [7] and [8] are approximate expressions, since [8] and [7] interchanged the order of integration and logarithm or the order of logarithm and the minimum function, while mathematically they are not interchangeable due to the non-linearity of the logarithm operation. The integration in (5.6) may be simplified by using special functions but no closed-form expressions can be derived due to its complexity.

5.2.4 Numerical Results

In this case, numerical examples of the BER and throughput in different scenarios will be presented. Without loss of generality, in the examples, we set $P_S = 1$, $\sigma_{\rm ra}^2 = \sigma_{\rm rc}^2 = \sigma_{\rm da}^2 = \sigma_{\rm dc}^2 = 1$, while $|h|^2$ and $|g|^2$ in the instantaneous transmission change with $\beta_1 = \frac{|h|^2}{\sigma_{\rm ra}^2+\sigma_{\rm rc}^2}$ and $\beta_2 = \frac{|g|^2}{\sigma_{\rm da}^2+\sigma_{\rm dc}^2}$ and Ω_1 and Ω_2 in the delay- and error-tolerant transmissions change with $\beta_1 = \frac{\Omega_1}{\sigma_{\rm ra}^2+\sigma_{\rm rc}^2}$ and $\beta_2 = \frac{\Omega_2}{\sigma_{\rm da}^2+\sigma_{\rm dc}^2}$. The values of β_1 and β_2 indicate how good the source-to-relay and relay-to-destination links are.

Figure 5.3 shows the maximum throughput using the optimized ρ for different values of β_1 and β_2. When β_1 is fixed in the legend, the X-axis corresponds to β_2, and when β_2 is fixed in the legend, the X-axis corresponds to β_1. In this case, one

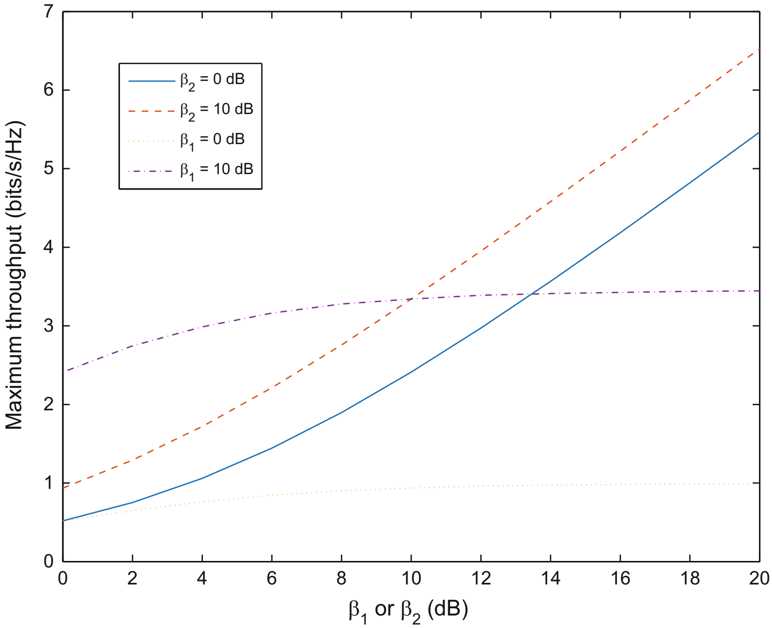

Fig. 5.3 Maximum throughput using optimum ρ vs. β_1 or β_2 when $\eta = 0.3$ in instantaneous transmission

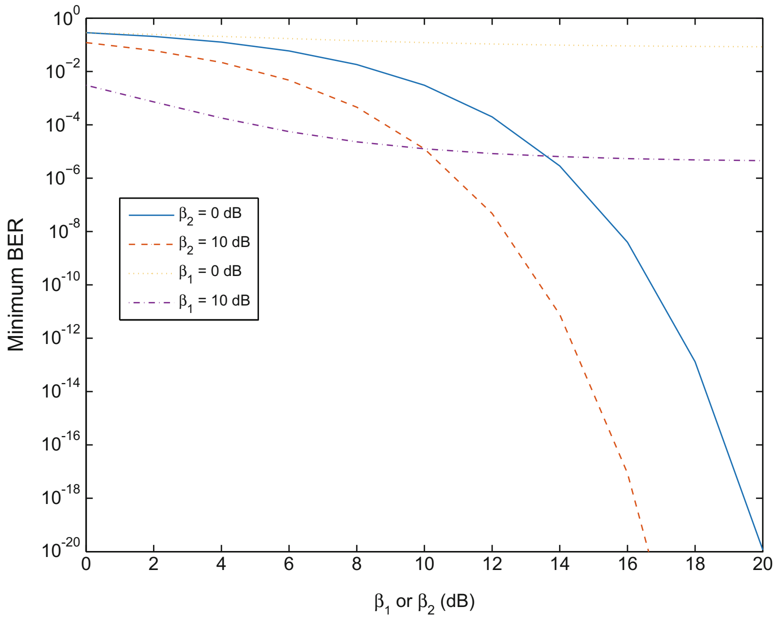

Fig. 5.4 Minimum BER using optimum ρ vs. β_1 or β_2 when $\eta = 0.3$ in instantaneous transmission

sees that the optimized throughput increases significantly with β_1, when β_2 is fixed to 0 and 10 dB, while the optimized throughput remains almost the same when β_2 increases and β_1 is fixed to 0 and 10 dB. Thus, the throughput is more sensitive to β_1. Figure 5.4 shows the minimum BER using the optimized ρ for different values of β_1 and β_2. Similarly, the BER is more sensitive to β_1 than to β_2. This indicates that the S-R link is more important than the R-D link in this case, as expected, as the S-R link not only determines the throughput or BER at the relay, but also determines the throughput or BER at the destination, via the harvested power.

Figure 5.5 shows the optimized value of ρ used to calculate the maximum throughput in Fig. 5.3. When β_2 is fixed to 0 dB or 10 dB, the optimum ρ does not change when β_1 increases. This agrees with the discussion before that the optimum ρ does not depend on $|h|^2$. When β_1 is fixed to 0 dB or 10 dB, the optimum ρ decreases with an increasing β_2, as less power needs to be harvested when the channel condition of the relay-to-destination link improves, under the same other conditions. Figure 5.6 gives the optimum ρ used to calculate the minimum BER in Fig. 5.4. Again, in general, the optimum ρ is more sensitive to β_2 than to β_1.

Figure 5.7 gives the optimized ρ for the maximum throughput for different β_1 and β_2 in delay- or error-tolerant transmission. It is interesting to note that in this case, when β_2 is fixed to 0 dB or 10 dB, the optimum ρ increases very slowly with β_1, very close to a constant as in the instantaneous transmission. However, the optimum ρ does decrease when β_2 increases, for fixed β_1. This implies to us

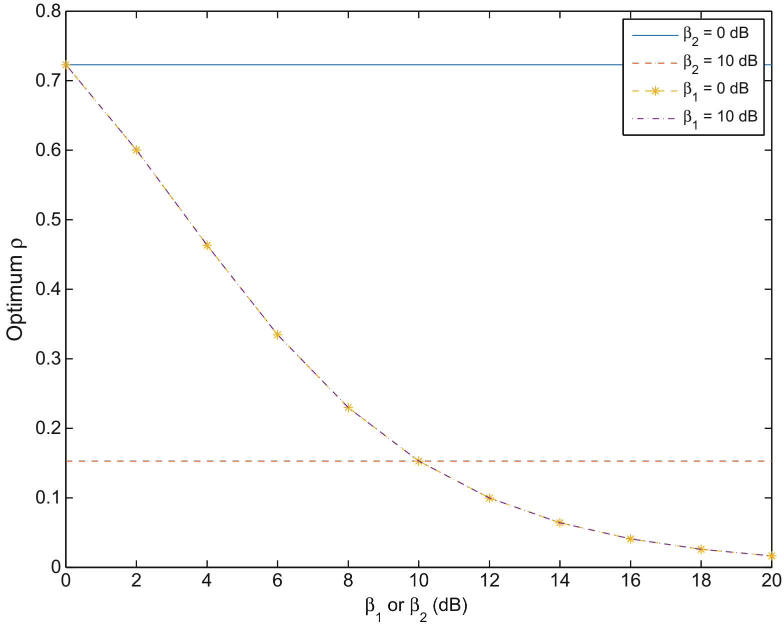

Fig. 5.5 The optimum ρ vs. β_1 or β_2 when $\eta = 0.3$ to achieve the maximum throughput in instantaneous transmission

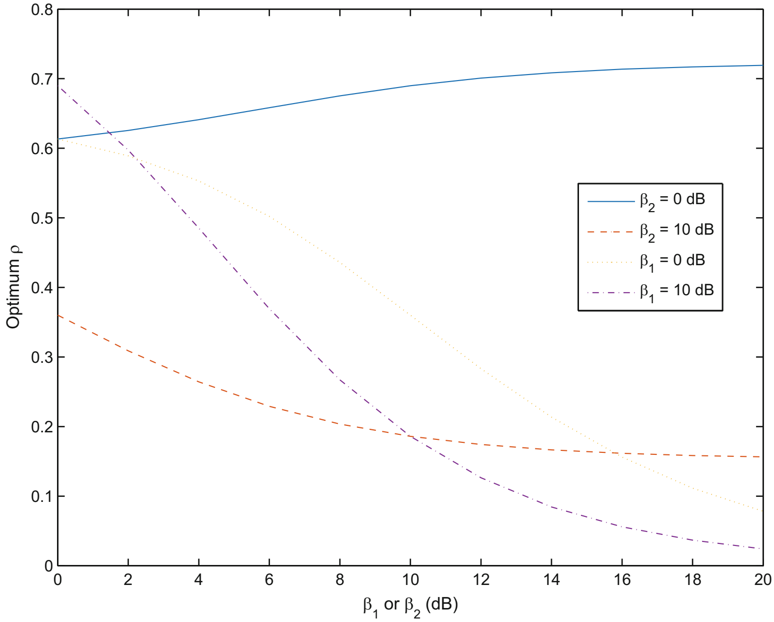

Fig. 5.6 The optimum ρ vs. β_1 or β_2 when $\eta = 0.3$ to achieve the minimum BER in instantaneous transmission

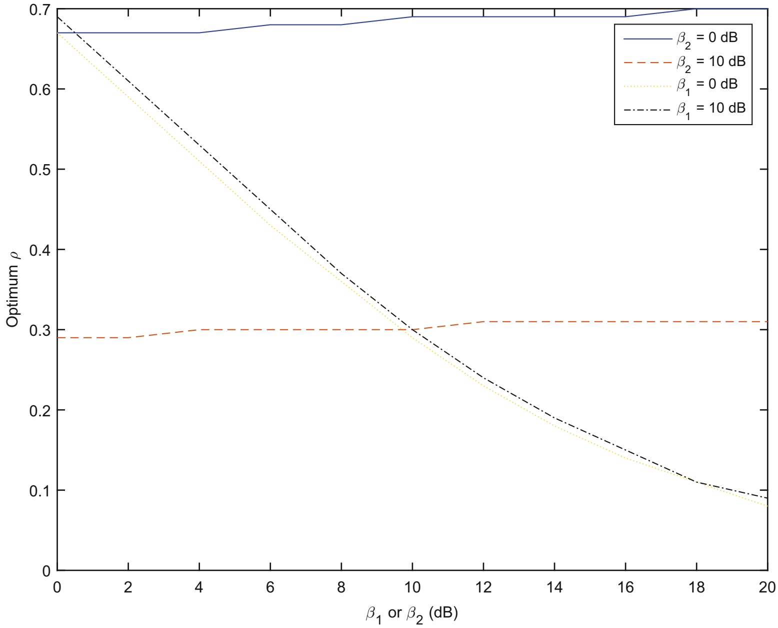

Fig. 5.7 The optimum ρ vs. β_1 or β_2 when $m_1 = m_2 = 2$ and $\eta = 0.3$ for the maximum throughput in delay-tolerant transmission

that in delay-tolerant transmission, the R-D link is more important than the S-R link. Figure 5.8 gives the optimum ρ for the minimum BER for different β_1 and β_2 in delay- or error-tolerant transmission. In this case, this optimum value changes significantly in most curves when β_1 or β_2 increase or decrease.

5.2.5 Conclusion

In this section, the throughput and BER expressions for DF relaying using PS have been analysed for Nakagami-m fading channels in two different transmission scenarios. Numerical results have shown that there does exist an optimum value of the PS factor in all the cases considered. For instantaneous transmission, the optimum value of ρ for maximum throughput does not depend on β_1 in this case. For delay- or error-tolerant transmissions, the relaying performance is less sensitive to η too. In addition, the optimum ρ that achieves maximum throughput is insensitive to β_1, while the optimum ρ for minimum BER is sensitive to both β_1 and β_2.

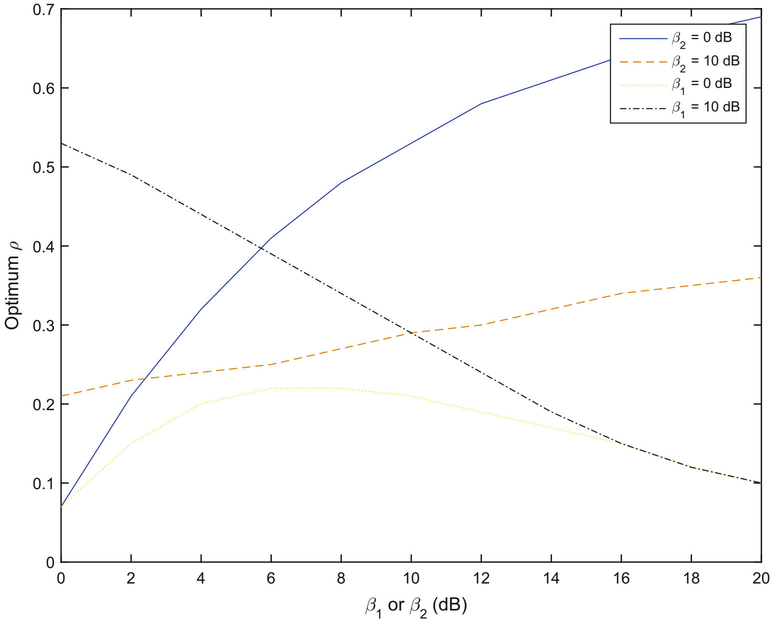

Fig. 5.8 The optimum ρ vs. β_1 or β_2 when $m_1 = m_2 = 2$ and $\eta = 0.3$ for the minimum BER in error-tolerant transmission

5.3 Energy Harvesting AF Relaying with Interference

5.3.1 Introduction

The AF protocol does not perform as well as the DF protocol but is simpler than the DF protocol. So it will be useful for applications where complexity is limited. Also, in a practical network, the relaying process may be subject to interference caused by other transmitters in the network. In this section, we will study the performance of energy harvesting AF relaying with interference. Again, we consider the PS scheme.

Some previous works on energy harvesting AF relaying exist. For example, reference [12] studied two energy harvesting AF schemes using PS and TS. Reference [13] studied a harvest-use structure, where the relay does not have energy storage capability and has to use the harvested energy immediately after it is harvested, for the optimal trade-off between harvesting time and relaying time. Reference [14] studied the optimal power allocation for energy harvesting AF, where relays can harvest energies from multiple source nodes and the total harvested energy was then allocated for transmissions of signals to different destinations. All these works consider Rayleigh fading. They did not consider the effect of interference either.

To provide more insights on various aspects of AF relaying using PS, in this section, the performance of AF relaying using PS is analysed by deriving the outage probability and the throughput in Nakagami-m fading channels, when both the relay and the destination suffer from interference. Both fixed-gain relaying and variable-gain AF relaying are studied. Using the derived expressions, the effects of different system parameters on the system performance are examined.

Again, consider a three-node system without a direct link between source and destination. For PS, a fraction of the received signal is harvested without any dedicated harvesting time. Thus, the transmission from the source to the relay takes $\frac{T}{2}$ seconds and the received information signal at the relay is given by

$$y_k^r = \sqrt{(1-\rho)P_s}ha + \sqrt{1-\rho}\sum_{i=1}^{N}\sqrt{P_i}h_i a_i + \sqrt{1-\rho}n_k^{\mathrm{ra}} + n_k^{\mathrm{rc}} \tag{5.7}$$

where N is the number of interfering sources at the relay, P_i is the transmission power of the i-th interferer, h_i is the fading gain from the i-th interferer to the considered relay, a_i is the transmitted BPSK bit of the i-th interferer and all the other symbols are defined as before. We assume Nakagami-m fading such that $|h_i|^2$, $i = 1, 2, \ldots, N$, are Gamma distributed with $f_{|h_i|^2}(x) = \left(\frac{m_{I1}}{\Omega_{I1}}\right)^{m_{I1}} \frac{x^{m_{I1}-1}}{\Gamma(m_{I1})} e^{-\frac{m_{I1}}{\Omega_{I1}}x}, x > 0$, where m_{I1} and Ω_{I1} are the m parameter and the average fading power from the interferer to the relay, respectively. They are assumed to be independent and identically distributed. Then, the harvested energy is given by $E_h = \eta\rho(P_s|h|^2 + \sum_{i=1}^{N} P_i|h_i|^2)\frac{T}{2}$.

Using the harvested energy, the received information is amplified and forwarded. The received signal at the destination is given by

$$y_k^d = \sqrt{P_r}agy_k^r + \sum_{j=1}^{N}\sqrt{Q_j}g_j b_j + n_k^{\mathrm{da}} + n_k^{\mathrm{dc}} \tag{5.8}$$

where $P_r = \frac{E_h}{T/2} = \eta\rho(P_s|h|^2 + \sum_{i=1}^{N} P_i|h_i|^2)$, Q_j is the transmission power of the j-th interferer to the destination, g_j is the fading gain from the j-th interferer to the destination, b_j is the transmitted BPSK bit of the j-th interferer and all other symbols are defined as before. The amplification factor depends on the method of AF relaying [15–17]. In fixed-gain relaying, a is a constant and without loss of generality, $a = 1$. In variable-gain relaying, one has $a = \frac{1}{\sqrt{(1-\rho)P_S|h|^2+(1-\rho)\sigma_{\mathrm{ra}}^2+\sigma_{\mathrm{rc}}^2}}$. We again assume Nakagami-m fading such that $|g_j|^2, j = 1, 2, \ldots, N$, are Gamma distributed with $f_{|g_j|^2}(x) = \left(\frac{m_{I2}}{\Omega_{I2}}\right)^{m_{I2}} \frac{x^{m_{I2}-1}}{\Gamma(m_{I2})} e^{-\frac{m_{I2}}{\Omega_{I2}}x}, x > 0$, where m_{I2} and Ω_{I2} are the m parameter and the average fading power in the link from the j-th interferer to the destination, respectively.

5.3.2 Outage

The outage probability is defined as the probability that the SINR is below a certain threshold γ_0 as $P_{\text{out}} = Pr\{\gamma < \gamma_0\}$. Denote $\gamma_2 = \frac{|g|^2}{\sum_{j=1}^{N} Q_j|g_j|^2+\sigma_{\text{da}}^2+\sigma_{\text{dc}}^2}$ and $\gamma_3 = \frac{|h|^2}{\sum_{i=1}^{N} P_i|h_i|^2+\sigma_{\text{ra}}^2+\sigma_{\text{rc}}^2/(1-\rho)}$. Using (5.8), the end-to-end signal-to-interference-plus-noise ratio (SINR) can be derived as

$$\gamma = \frac{P_S a^2 \gamma_2 \gamma_3}{a^2\gamma_2 + \frac{1}{\eta\rho[(1-\rho)\sum_{i=1}^{N} P_i|h_i|^2+(1-\rho)\sigma_{\text{ra}}^2+\sigma_{\text{rc}}^2](P_S|h|^2+\sum_{i=1}^{N} P_i|h_i|^2)}}. \tag{5.9}$$

Compared with the end-to-end SINR for the conventional relaying, the end-to-end SINR for energy harvesting relaying has an additional term of $(P_S|h|^2 + \sum_{i=1}^{N} P_i|h_i|^2)$ multiplied with the second term in the denominator, which has caused complexity.

The outage probability for fixed-gain relaying using PS can be derived as

$$\begin{aligned} P_{\text{out}}^{\text{PS}-\text{FG}} &= 1 - \left(\frac{m_{I1}}{P_{I1}\Omega_{I1}}\right)^{Nm_{I1}} \left(\frac{m_1}{P_S\Omega_1}\right)^{m_1} \left(\frac{m_{I2}}{Q_{I2}\Omega_{I2}}\right)^{Nm_{I2}} \frac{1}{\Gamma(Nm_{I1})\Gamma(m_1)\Gamma(Nm_{I2})} \\ &\sum_{l=0}^{m_2-1}\sum_{l'=0}^{l} \frac{(m_2/\Omega_2)^l \binom{l'}{l} (\sigma_{\text{da}}^2+\sigma_{\text{dc}}^2)^{l-l'}(Nm_{I2}+l'-1)!}{l!} \\ &\cdot \int_0^\infty \int_{\gamma_0 z+\gamma_0\sigma_{\text{ra}}^2+\gamma_0\sigma_{\text{rc}}^2/(1-\rho)}^\infty e^{-\frac{m_2(\sigma_{\text{da}}^2+\sigma_{\text{dc}}^2)}{\Omega_2}X_{PS-FG}(y,z)-\frac{m_1}{P_s\Omega_1}y-\frac{m_{I1}}{P_{I1}\Omega_{I1}}z} \\ &\cdot \frac{(X_{PS-FG}(y,z))^l y^{m_1-1} z^{Nm_{I1}-1}}{\left(\frac{m_{I2}}{Q_{I2}\Omega_{I2}} + \frac{m_2 X_{\text{PS}-\text{FG}}(y,z)}{\Omega_2}\right)^{Nm_{I2}+l'}} dydz. \end{aligned} \tag{5.10}$$

where $X_{PS-FG}(y,z) = \frac{\gamma_0}{\eta\rho(1-\rho)}\frac{1}{(y+z)}\frac{1}{(y-\gamma_0 z-\gamma_0\sigma_{ra}^2-\gamma_0\sigma_{rc}^2/(1-\rho))}$.

Similarly, if variable-gain relaying is used, the outage probability is derived as

$$\begin{aligned} P_{\text{out}}^{\text{PS}-\text{VG}} &= 1 - \left(\frac{m_{I1}}{P_{I1}\Omega_{I1}}\right)^{Nm_{I1}} \left(\frac{m_1}{P_S\Omega_1}\right)^{m_1} \left(\frac{m_{I2}}{Q_{I2}\Omega_{I2}}\right)^{Nm_{I2}} \frac{1}{\Gamma(Nm_{I1})\Gamma(m_1)\Gamma(Nm_{I2})} \\ &\sum_{l=0}^{m_2-1}\sum_{l'=0}^{l} \frac{(m_2/\Omega_2)^l \binom{l'}{l} (\sigma_{\text{da}}^2+\sigma_{\text{dc}}^2)^{l-l'}(Nm_{I2}+l'-1)!}{l!} \\ &\cdot \int_0^\infty \int_{\gamma_0 z+\gamma_0\sigma_{\text{ra}}^2+\gamma_0\sigma_{\text{rc}}^2/(1-\rho)}^\infty e^{-\frac{m_2(\sigma_{\text{da}}^2+\sigma_{\text{dc}}^2)}{\Omega_2}X_{PS-VG}(y,z)-\frac{m_1}{P_s\Omega_1}y-\frac{m_{I1}}{P_{I1}\Omega_{I1}}z} \\ &\cdot \frac{(X_{\text{PS}-\text{VG}}(y,z))^l y^{m_1-1} z^{Nm_{I1}-1}}{\left(\frac{m_{I2}}{Q_{I2}\Omega_{I2}} + \frac{m_2 X_{\text{PS}-\text{VG}}(y,z)}{\Omega_2}\right)^{Nm_{I2}+l'}} dydz \end{aligned} \tag{5.11}$$

where $X_{\mathrm{PS-VG}}(y,z) = \frac{\gamma_0}{\eta\rho(1-\rho)} \frac{(1-\rho)y+(1-\rho)\sigma_{\mathrm{ra}}^2+\sigma_{\mathrm{rc}}^2}{(y+z)(y-\gamma_0 Z_1-\gamma_0\sigma_{\mathrm{ra}}^2-\gamma_0\sigma_{\mathrm{rc}}^2/(1-\rho))}$. The detailed derivation can be found in [18].

5.3.3 *Throughput*

Let R be a fixed transmission rate that the source needs to satisfy such that $R = \log_2(1+\gamma_0)$. Then, one has $\gamma_0 = 2^R - 1$. For PS, the throughput can be derived as

$$\tau = (1-P_{\mathrm{out}})R\frac{T/2}{T} = \frac{R}{2}(1-P_{\mathrm{out}}) \tag{5.12}$$

Using $P_{\mathrm{out}}^{\mathrm{PS-FG}}$ in (5.10) and $P_{\mathrm{out}}^{\mathrm{PS-VG}}$ in (5.11) to replace P_{out} in (5.12), the throughput for energy harvesting relaying using PS can be derived.

5.3.4 *Numerical Results*

In this subsection, the effects of some important system parameters are examined by showing relevant numerical examples. In these examples, we set $\sigma_{\mathrm{ra}}^2 = \sigma_{\mathrm{rc}}^2 = \sigma_{\mathrm{da}}^2 = \sigma_{\mathrm{dc}}^2 = 1$, $P_S = P_{I1} = Q_{I2} = \Omega_{I1} = \Omega_{I2} = 1$, while Ω_1 and Ω_2 vary with the average SINR of the source-to-relay link and the average SINR of the relay-to-destination link defined as $\Delta_1 = \frac{\Omega_1}{NP_{I1}\Omega_{I1}+\sigma_{\mathrm{ra}}^2+\sigma_{\mathrm{rc}}^2}$ and $\Delta_2 = \frac{\Omega_2}{NQ_{I2}\Omega_{I2}+\sigma_{\mathrm{ra}}^2+\sigma_{\mathrm{rc}}^2}$, respectively.

Figures 5.9, 5.10, 5.11, 5.12, 5.13 show the throughput of energy harvesting relaying using PS versus ρ under different conditions. In these cases considered, the throughput always increases and the rate of increase becomes small, when the value of ρ increases. When $\rho = 0.8$, the throughput is very close to the maximum it can be, indicating that there is greater flexibility in the choice of ρ. Also, the sensitivity of the throughput to ρ is small, as the value of throughput ranges between 0.9 and 1 in most cases in Figs. 5.9, 5.10, 5.11, 5.12, 5.13. One also sees from these figures that fixed-gain relaying has larger throughput than variable-gain relaying, the throughput increases when η increases, N decreases, R increases, the SINR increases or the m parameter increases. The throughput is more sensitive to N, R, Δ_1 and m_1 than to η, Δ_2 and the relaying method.

5.3.5 *Conclusion*

The performance of energy harvesting AF relaying has been evaluated in terms of the outage and the throughput for Nakagami-m fading with interference. Using these results, the effects of the PS factor ρ, the conversion efficiency of harvester η, the number of interferers N, the required fixed transmission rate R, the SINR of different hops and the m parameter on the throughput performance have been examined.

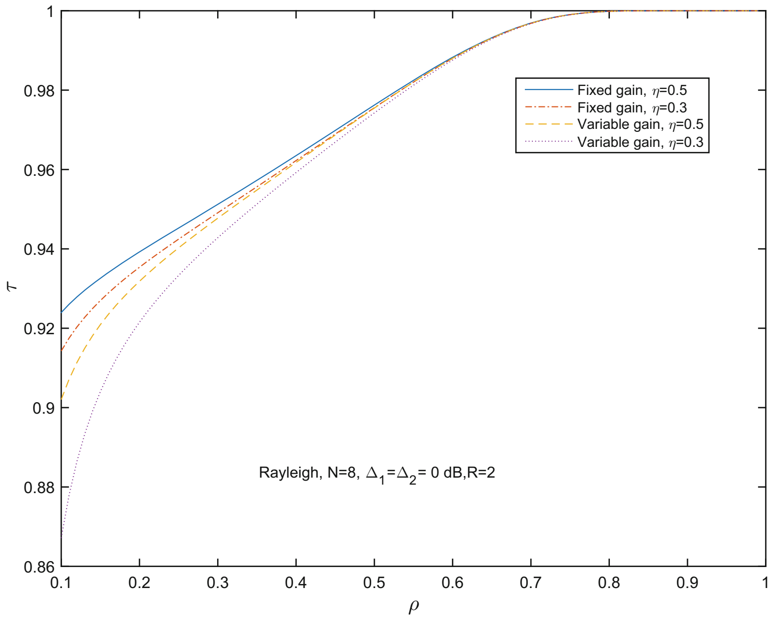

Fig. 5.9 Throughput vs. ρ for different values of η using PS energy harvesting when $N = 8$, $\Delta_1 = \Delta_2 = 0\,\text{dB}$, $R = 2\,\text{bits/s/Hz}$ in Rayleigh fading channels

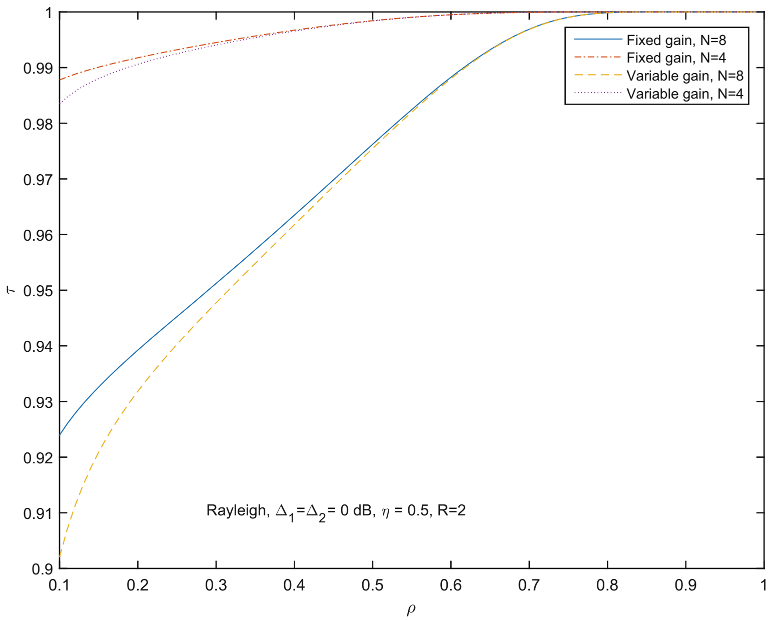

Fig. 5.10 Throughput vs. ρ for different values of N using PS energy harvesting when $\eta = 0.5$, $\Delta_1 = \Delta_2 = 0\,\text{dB}$, $R = 2\,\text{bits/s/Hz}$ in Rayleigh fading channels

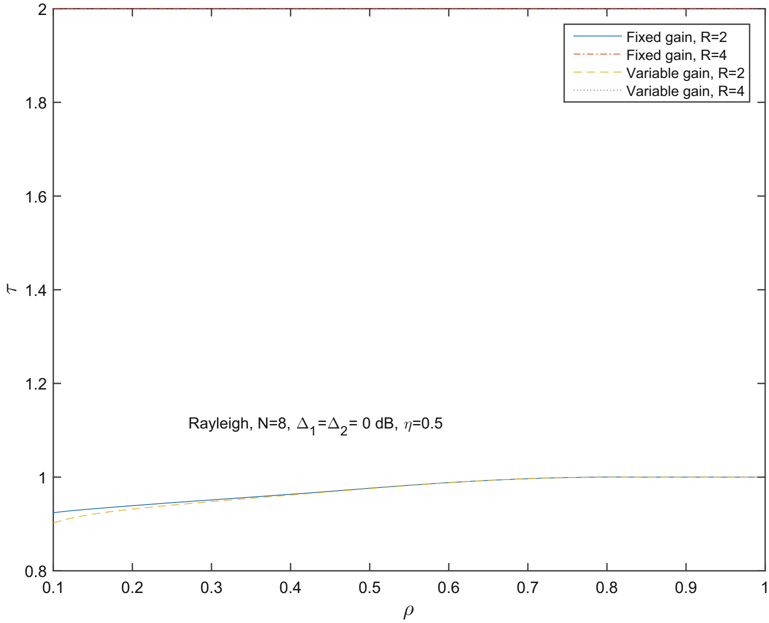

Fig. 5.11 Throughput vs. ρ for different values of R using PS energy harvesting when $N = 8$, $\Delta_1 = \Delta_2 = 0\,\text{dB}$, $\eta = 0.5$ in Rayleigh fading channels

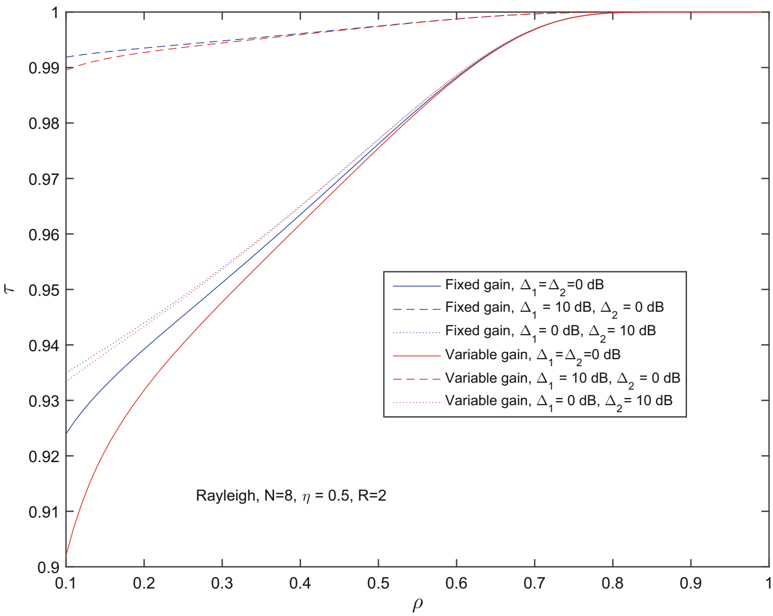

Fig. 5.12 Throughput vs. ρ for different values of Δ_1 and Δ_2 using PS energy harvesting when $N = 8$, $\eta = 0.5$, $R = 2\,\text{bits/s/Hz}$ in Rayleigh fading channels

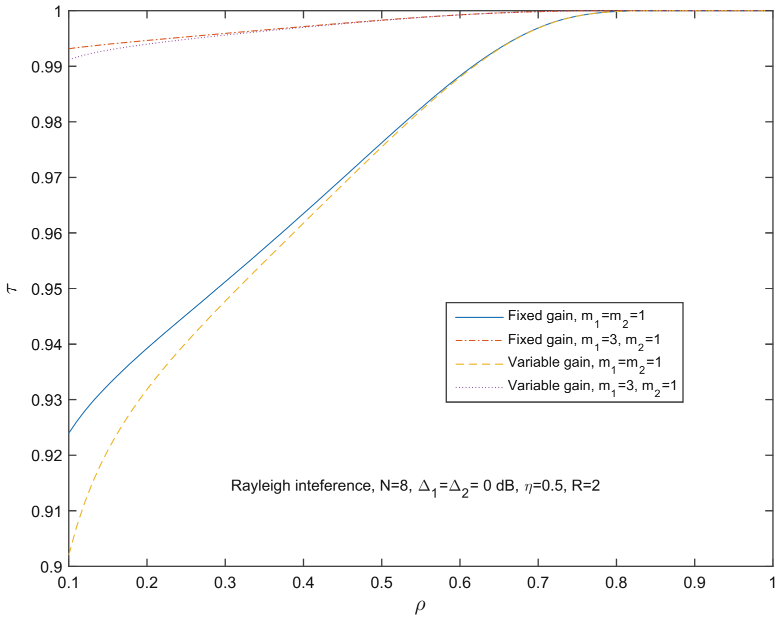

Fig. 5.13 Throughput vs. ρ for different values of m_1 using PS energy harvesting when $N = 8$, $\Delta_1 = \Delta_2 = 0$ dB, $R = 2$ bits/s/Hz, $\eta = 0.5$ and other channels suffer from Rayleigh fading

Numerical results show that PS is not sensitive to energy harvesting and that the throughput is more sensitive to N, R, Δ_1 and m_1 than to η, Δ_2 and the relaying method. Using these results, one can choose appropriate parameters for different application environments.

5.4 Design of New Energy Harvesting Relaying Protocol

5.4.1 Introduction

The above two sections and most previous works on energy harvesting relaying in the literature [6–14] have assumed energy harvesting relaying where the source transfers wireless energy to the relay in the first phase of broadcasting. More specifically, the conventional energy harvesting relaying protocol has two phases. In the first broadcasting phase, the source transmits signal to the relay for energy harvesting as well as information delivery. In the second relaying phase, the relay uses the harvested energy to forward the signal to the destination. This protocol provides an effective solution to energy harvesting relaying. However, note that in the second relaying phase when the relay uses the harvested energy to forward the signal, the signal is still broadcast by the relay to the destination. Thus, the conventional energy harvesting protocol can be further improved by allowing the

Fig. 5.14 Comparison of conventional energy harvesting relaying and new energy harvesting relaying

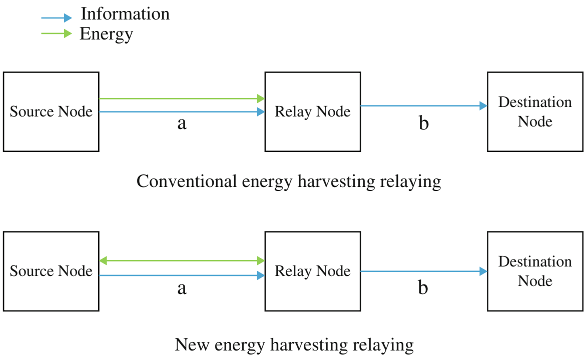

source to harvest energy from the relay transmitting in the second relaying phase to maximize the energy use. Figure 5.14 compares the conventional energy harvesting relaying with the new energy harvesting relaying schemes. One sees that in the new schemes the relay harvests energy from the source in the broadcasting phase and the source harvests energy from the relay in the relaying phase. In the conventional scheme, only the relay harvests energy from the source in the broadcasting phase.

In this work, we will study the performance of the new energy harvesting relaying protocol using AF as an example, where in the relaying phase, the relay transmits information to the destination while the source harvests energy from this transmission. In this case, we consider both TS and PS energy harvesting schemes. Before we move on to the analysis, a few assumptions need to be laid out. Again, consider a three-node relaying system without direct link between the source and the destination. Assume that both the source and the relay are equipped with energy harvesters. To illustrate the performance gain of the new protocol, we consider static AWGN channels without fading but with large-scale path loss. Also, assume that there are E_t joules of total energy initially available at the source and that the whole relaying transmission takes T seconds that includes broadcasting, relaying and energy harvesting. The system works as follows.

For TS, the relay receives energy from the source for αT seconds followed by information reception from the source for $\frac{1-\alpha}{2}T$ seconds, in the first broadcasting phase. The received signal at the relay can be given by

$$y_k^r = \sqrt{P_s}\frac{h}{\sqrt{d_{\text{sr}}^m}}a + n_k^{\text{ra}} + n_k^{\text{rc}} \tag{5.13}$$

where d_{sr} is the distance between source and relay, m is the path loss exponent and all the other symbols are defined as before. Thus, compared with the signals we used before, we have stated the large-scale path loss explicitly as d_{sr}^m. Using this received signal, the first period of time is used for energy harvesting to give the harvested energy at the relay as $E_{\text{hr}} = \eta P_s \frac{h^2}{d_{\text{sr}}^m}\alpha T$.

In the second relaying phase, the relay node will forward the signal from the source to the destination for $\frac{1-\alpha}{2}T$ seconds and the received signal at the destination can be given by

$$y_k^d = \frac{g}{\sqrt{d_{\mathrm{rd}}^m}}\sqrt{P_r}dy_k^r + n_k^{\mathrm{da}} + n_k^{\mathrm{dc}} \tag{5.14}$$

where d_{rd} is the distance between relay and destination, $P_r = \frac{E_{\mathrm{hr}}}{\frac{1-\alpha}{2}T} = \frac{2\alpha\eta}{1-\alpha}P_s\frac{h^2}{d_{\mathrm{sr}}^m}$ is the transmission power of the relay, dy_k^r is the normalized transmitted signal, normalized with respect to the average power of y_k^r as $d = \frac{1}{\sqrt{P_s\frac{h^2}{d_{\mathrm{sr}}^m}+\sigma_{\mathrm{ra}}^2+\sigma_{\mathrm{rc}}^2}}$.

Unlike the conventional energy harvesting relaying protocol, in the new protocol, the source also harvests energy from the signal transmitted by the relay. Thus, during the second relaying phase, the received signal at the source is given by

$$y_k^s = \frac{h}{\sqrt{d_{\mathrm{sr}}^m}}\sqrt{P_r}dy_k^r + n_k^{\mathrm{sa}} \tag{5.15}$$

where we have used the channel reciprocity such that the channel gain h and the distance d_{sr} do not change for the S-R or R-S links and n_k^{sa} is the AWGN at the source. In this case, the harvested energy at the source is $E_{\mathrm{hs}} = \eta\frac{P_rP_sd^2h^4}{d_{\mathrm{sr}}^{2m}}\cdot\frac{(1-\alpha)T}{2}$. This equals to $E_{\mathrm{hs}} = \eta^2\alpha\frac{P_s^2(h^2/d_{\mathrm{sr}}^m)^3T}{P_sh^2/d_{\mathrm{sr}}^m+\sigma_{\mathrm{ra}}^2+\sigma_{\mathrm{rc}}^2}$.

For PS, since there is no dedicated harvesting time, in this case, the source first transmits the signal to the relay for $\frac{T}{2}$ seconds, part of which is received at the relay for information decoding as

$$y_k^r = \sqrt{(1-\rho)P_s}\frac{h}{\sqrt{d_{\mathrm{sr}}^m}}a + \sqrt{1-\rho}n_k^{\mathrm{ra}} + n_k^{\mathrm{rc}} \tag{5.16}$$

and part of which is harvested by the relay as $E_{\mathrm{hr}} = \eta\rho P_s\frac{h^2}{d_{\mathrm{sr}}^m}\frac{T}{2}$. All the symbols are defined as before.

In the second relaying phase, the relay will use its harvested energy to forward the received signal. Then, the received signal at the destination becomes

$$y_k^d = \frac{g}{\sqrt{d_{\mathrm{rd}}^m}}\sqrt{P_r}dy_k^r + n_k^{\mathrm{da}} + n_k^{\mathrm{dc}} \tag{5.17}$$

where in this case $P_r = \frac{E_{\mathrm{hr}}}{T/2} = \eta\rho P_s\frac{h^2}{d_{\mathrm{sr}}^m}$.

Also, unlike the conventional relaying protocol, in the second relaying phase of the new protocol, the source needs to harvest energy from the signal transmitted by the relay so its received signal is

$$y_k^s = \frac{h}{\sqrt{d_{\mathrm{sr}}^m}}\sqrt{P_r}dy_k^r + n_k^{\mathrm{sa}} \tag{5.18}$$

and the harvested energy from this received signal is derived as $E_{\rm hs} = \eta^2\rho(1-\rho)\frac{P_s^2(h^2/d_{\rm sr}^m)^3T/2}{P_sh^2/d_{\rm sr}^m+\sigma_{\rm ra}^2+\sigma_{\rm rc}^2}$. Next, we consider two strategies of using this newly harvested energy. In the first strategy, all the harvested energies at the source node during different relaying transmissions will be stored until all the transmissions are finished. The stored energy is then used to conduct more relaying transmissions. In the second strategy, instead of storing all harvested energy until all the relaying transmissions are finished, the harvested energy will be used immediately in the next relaying transmission to increase its transmission power and therefore its transmission rate. This strategy has the advantages of requiring smaller energy storage at the source node as well as improving the quality of each relay transmission.

5.4.2 Conventional Protocol

For the conventional TS relaying protocol, the source transmits the signal for a duration of $\alpha T + \frac{1-\alpha}{2}T$ with a transmission power of P_s, where the first part is the dedicated energy transfer time and the second part is the extra information transmission time. Thus, each relaying transmission will assume an energy of $E_i = \left[\alpha T + \frac{1-\alpha}{2}T\right]P_s$. Thus, given a total energy of E_t at the beginning, the total number of relaying transmissions the source can perform using the conventional TS relaying protocol can be calculated as $K_{\rm TS}^{\rm Con} = \frac{E_t}{E_i} = \frac{E_t}{P_sT}\frac{2}{1+\alpha}$.

For TS, the end-to-end signal-to-noise ratio (SNR) can be derived using the received signal expression as $\gamma_{\rm TS} = \frac{P_s\gamma_d\gamma_r a^2}{\gamma_d d^2+\frac{(1-\alpha)d_{\rm sr}^m}{2\alpha\eta P_s h^2(\sigma_{\rm rc}^2+\sigma_{\rm ra}^2)}}$, where $\gamma_d = \frac{g^2}{d_{\rm rd}^m(\sigma_{\rm da}^2+\sigma_{\rm dc}^2)}$ and $\gamma_r = \frac{h^2}{d_{\rm sr}^m(\sigma_{\rm ra}^2+\sigma_{\rm rc}^2)}$ are the hop SNRs similar to before but with large-scale path loss now. Thus, the total transmission rate or throughput in all relaying transmissions can be shown as

$$C_{\rm TS}^{\rm Con} = K_{\rm TS}^{\rm Cov}\cdot\log_2(1+\gamma_{\rm TS})\frac{1-\alpha}{2}. \tag{5.19}$$

The calculation for PS is very similar. In the conventional PS relaying protocol, each relay transmission consumes an energy of $E_i = \frac{T}{2}P_s$ and thus, given the initial energy of E_t, the total number of relaying transmissions is then $K_{\rm PS}^{\rm Con} = \frac{2E_t}{P_sT}$.

Also, for PS, the end-to-end SNR can be derived as $\gamma_{\rm PS}=\frac{P_s\gamma_d\gamma_p a^2}{\gamma_d d^2+\frac{d_{\rm sr}^m}{(1-\rho)[\sigma_{\rm ra}^2+\sigma_{\rm rc}^2/(1-\rho)]\eta\rho P_s h^2}}$, where $\gamma_p = \frac{h^2}{d_{\rm sr}^m[\sigma_{\rm ra}^2+\sigma_{\rm rc}^2/(1-\rho)]}$ and other symbols are defined as before. Finally, the total transmission rate or throughput of all relaying transmissions using the conventional PS relaying protocol is

$$C_{\rm PS}^{\rm Con} = \frac{K_{\rm PS}^{\rm Con}}{2}\log_2(1+\gamma_{\rm PS}). \tag{5.20}$$

5.4.3 First Strategy of Using New Energy

Consider the first strategy where the harvested energies at the source will be stored until all relaying transmissions are finished. Then, they will be used to transmit more data. In this case, the new total number of relaying transmissions can be derived as $K_{\text{TS}}^{\text{New}} = \left\lceil \frac{E_t/(P_s T)}{\frac{1+\alpha}{2} - \eta^2\alpha \frac{P_s^2(h^2/d_{\text{sr}}^m)^3 T}{P_s h^2/d_{\text{sr}}^m + \sigma_{\text{ra}}^2 + \sigma_{\text{rc}}^2}} \right\rceil$, where $\lceil\cdot\rceil$ is the rounding function to get an integer and $\frac{1+\alpha}{2} > \eta^2\alpha \frac{P_s^2(h^2/d_{\text{sr}}^m)^3 T}{P_s h^2/d_{\text{sr}}^m + \sigma_{\text{ra}}^2 + \sigma_{\text{rc}}^2}$ which is always the case as the harvested energy is positive. Thus, since the number of relaying transmissions is increased while the throughput for each transmission is the same as conventional scheme, one has the total throughput in the first strategy as

$$C_{\text{TS}}^{\text{New1}} = K_{\text{TS}}^{\text{New}} \cdot \log_2(1 + \gamma_{\text{TS}}) \frac{1-\alpha}{2}. \tag{5.21}$$

For PS, the derivation is similar. The new number of total relaying transmissions using PS is calculated as $K_{\text{PS}}^{\text{New}} = \left\lceil \frac{2E_t/(P_s T)}{1 - \eta^2\rho(1-\rho) \frac{P_s^2(h^2/d_{\text{sr}}^m)^3 T/2}{P_s h^2/d_{\text{sr}}^m + \sigma_{\text{ra}}^2 + \sigma_{\text{rc}}^2}} \right\rceil$, where $1 > \eta^2\rho(1-\rho) \frac{P_s^2(h^2/d_{\text{sr}}^m)^3 T/2}{P_s h^2/d_{\text{sr}}^m + \sigma_{\text{ra}}^2 + \sigma_{\text{rc}}^2}$ and thus one has the new total throughput as

$$C_{\text{PS}}^{\text{New1}} = \frac{K_{\text{PS}}^{\text{New}}}{2} \log_2(1 + \gamma_{\text{PS}}). \tag{5.22}$$

5.4.4 Second Strategy of Using New Energy

Consider the second strategy. In this case, the extra energy harvested by the source will be used in the next relaying transmission to save battery capacity. Because of this, an iterative process is used as

$$\begin{aligned}
P_s^{(i+1)} &= \frac{E_t/K_{\text{TS}}^{\text{Con}} + E_{\text{hs}}^{(i)}}{T} \frac{2}{1+\alpha} \\
\gamma_{\text{TS}}^{i+1} &= \frac{P_s^{(i+1)}\gamma_d\gamma_r}{\gamma_d + \frac{(1-\alpha)d_{\text{sr}}^m (P_s^{(i+1)} \frac{h^2}{d_{\text{sr}}^m} + \sigma_{\text{ra}}^2 + \sigma_{\text{rc}}^2)}{2\alpha\eta P_s^{(i+1)} h^2 (\sigma_{\text{ra}}^2 + \sigma_{\text{rc}}^2)}} \\
E_{\text{hs}}^{(i+1)} &= \eta^2\alpha \frac{(P_s^{(i)})^2 (h^2/d_{\text{sr}}^m)^3 T}{P_s^{(i)} h^2/d_{\text{sr}}^m + \sigma_{\text{ra}}^2 + \sigma_{\text{rc}}^2}.
\end{aligned} \tag{5.23}$$

where $i = 1, 2, \ldots, K_{\mathrm{TS}}^{\mathrm{Con}}$ denote the i-th transmission, $E_{\mathrm{hs}}^{1} = 0$ and $P_s^1 = P_s$ as the initial conditions. Thus, the new total throughput is derived as

$$C_{\mathrm{TS}}^{\mathrm{New2}} = \sum_{i=1}^{K_{\mathrm{TS}}^{\mathrm{Con}}} \log_2(1 + \gamma_{\mathrm{TS}}^{(i)})\frac{1-\alpha}{2}. \tag{5.24}$$

For PS, one has

$$\begin{aligned}
P_s^{(i+1)} &= \frac{2(E_t/K_{\mathrm{PS}}^{\mathrm{Con}} + E_{\mathrm{hs}}^{(i)})}{T} \\
\gamma_{\mathrm{PS}}^{i+1} &= \frac{P_s^{(i+1)}\gamma_d\gamma_p}{\gamma_d + \frac{d_{\mathrm{sr}}^m(P_s^{(i+1)}\frac{h^2}{d_{\mathrm{sr}}^m}+\sigma_{\mathrm{ra}}^2+\sigma_{\mathrm{rc}}^2)}{[(1-\rho)\sigma_{\mathrm{ra}}^2+\sigma_{\mathrm{rc}}^2]\eta\rho P_s^{(i+1)}h^2}} \\
E_{\mathrm{hs}}^{(i+1)} &= \eta^2\rho(1-\rho)\frac{(P_s^{(i)})^2(h^2/d_{\mathrm{sr}}^m)^3 T/2}{P_s^{(i)}h^2/d_{\mathrm{sr}}^m + \sigma_{\mathrm{ra}}^2 + \sigma_{\mathrm{rc}}^2}.
\end{aligned} \tag{5.25}$$

and the new total throughput is therefore

$$C_{\mathrm{PS}}^{\mathrm{New2}} = \sum_{i=1}^{K_{\mathrm{PS}}^{\mathrm{Con}}} \log_2(1 + \gamma_{\mathrm{PS}}^{(i)})\frac{1}{2}. \tag{5.26}$$

5.4.5 Numerical Results

In this subsection, numerical examples are given to show the performance of the new protocol, where the values of α and ρ are calculated by maximizing the throughput of a single transmission $\log_2(1+\gamma_{\mathrm{TS}})\frac{1-\alpha}{2}$ or $\log_2(1+\gamma_{\mathrm{PS}})\frac{1}{2}$, respectively. For fixed h, the value of $\frac{h^2}{d_{\mathrm{sr}}^m}$ is determined by d_{sr}. Thus, in the following, we examine the effects of P_s, η, d_{sr} and $\sigma_{\mathrm{ra}}^2 + \sigma_{\mathrm{rc}}^2$ on the performance gain. Other parameters are set as $E_t = 100\,\mathrm{J}$, $T = 1\,\mathrm{s}$, $\sigma_{\mathrm{ra}}^2 = \sigma_{\mathrm{rc}}^2 = \sigma_{\mathrm{da}}^2 = \sigma_{\mathrm{dc}}^2 = \sigma^2$, $m = 2.7$ and $h = g = 1$. These parameters can be changed to evaluate more conditions. The path loss exponent $m = 2.7$ corresponds to an urban cellular environment [19]. The channel gains $h = g = 1$ is chosen such that the operating SNR will be from 10 to 20 dB without path loss, when σ^2 is from 0.01 to 0.1 as examined in this work. The choices of distances are for illustration purpose only. The performance gain examined in the following figures is calculated as the difference between the total throughput of new and conventional protocols normalized by that of the conventional protocol.

Figure 5.15 shows the performance gain vs. P_s. Several observations can be made. First, since the gain is always positive, the new protocol outperforms the

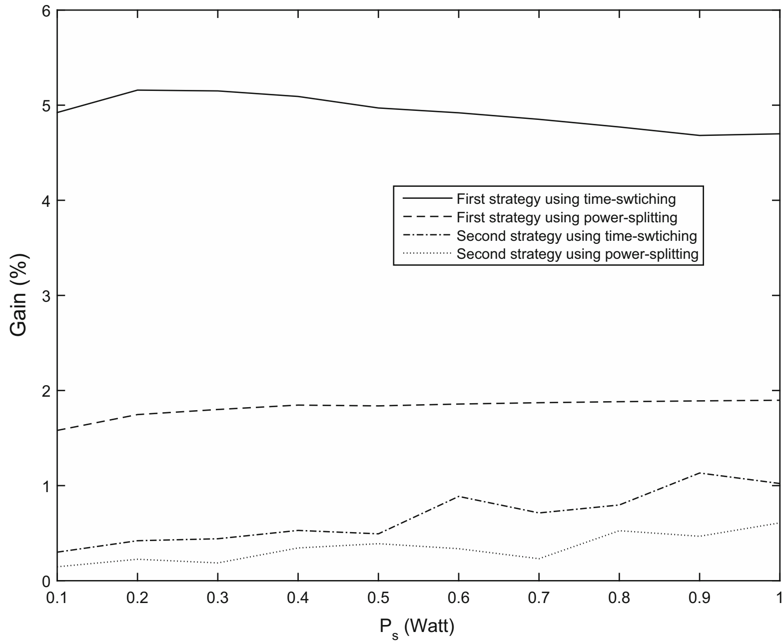

Fig. 5.15 Performance gain vs. P_s when $d_{\text{sr}} = 1.2\,\text{m}$, $d_{\text{rd}} = 1.2\,\text{m}$, $\eta = 0.5$ and $\sigma^2 = 0.01$

conventional protocol, as expected, as the source node harvests extra energy in the relaying phase. Second, the new protocol using the first strategy has a larger performance gain than that using the second strategy at the cost of requiring a larger capacity for energy storage. Third, the TS energy harvesting has a larger gain than the PS energy harvesting, as PS normally harvests less energy than TS.

Figure 5.16 shows the gain vs. η. One sees that the performance gain increases when η increases. Figure 5.17 shows the gain vs. d_{sr}. In this case, the performance gain decreases when d_{sr} increases. Also, compared with Fig. 5.16, the rate of change in Fig. 5.17 is much higher than that in Fig. 5.16. Again, the first strategy using TS has the largest gain. Figure 5.18 shows the gain vs. σ^2. In this case, the gain increases when σ^2 increases, except when the first strategy is used with PS.

5.4.6 *Conclusion*

From this section, one concludes that the distance d_{sr} has the largest effect on the performance gain, followed by the conversion efficiency η. To increase the performance gain of the new protocol, one needs to choose a large η or a small d_{sr}. Also, TS is preferred to PS, as it produces larger gains. Note that the above

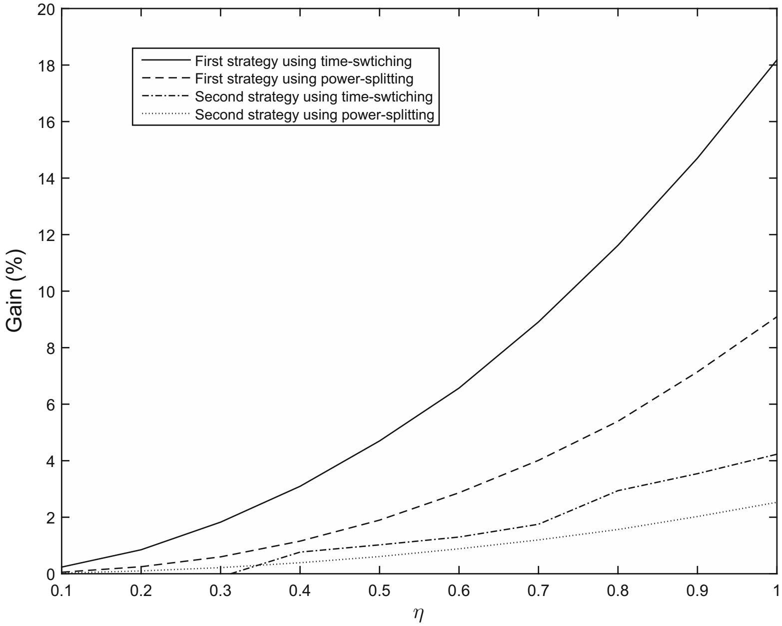

Fig. 5.16 Performance gain vs. η when $P_s = 1\,\text{W}$, $d_{\text{sr}} = 1.2\,\text{m}$, $d_{\text{rd}} = 1.2\,\text{m}$ and $\sigma^2 = 0.01$

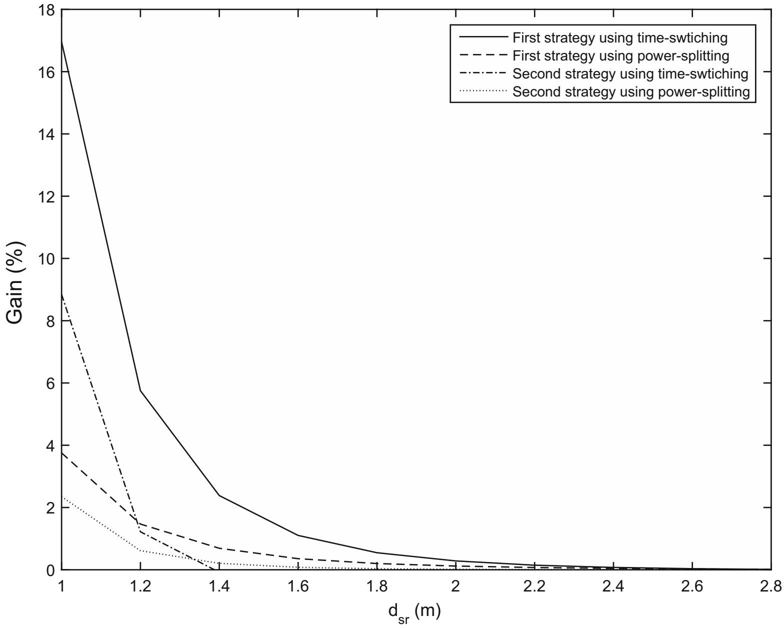

Fig. 5.17 Performance gain vs. d_{sr} when $P_s = 1\,\text{W}$, $d_{\text{rd}} = 3 - d_{\text{sr}}$, $\eta = 0.5$ and $\sigma^2 = 0.01$

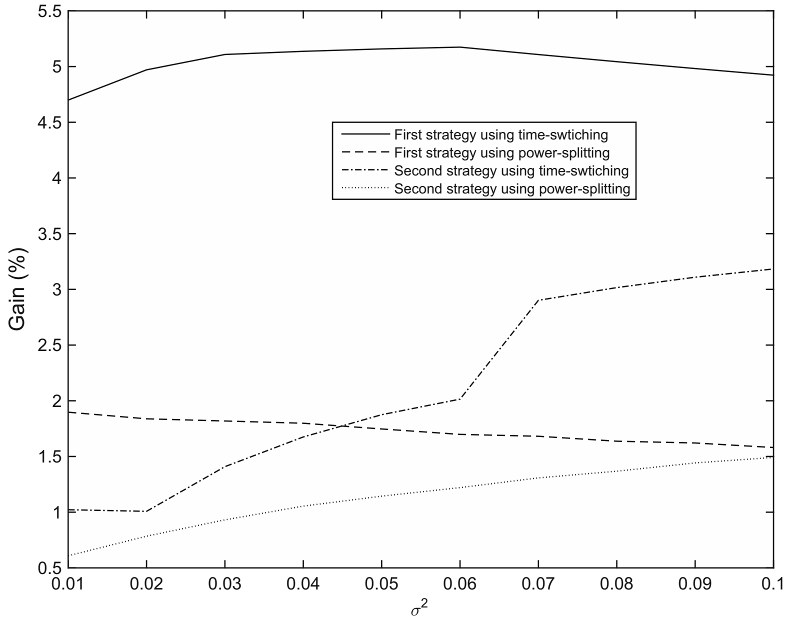

Fig. 5.18 Performance gain vs. σ^2 when $P_s = 1\,\mathrm{W}$, $d_{\mathrm{sr}} = 1.2\,\mathrm{m}$, $d_{\mathrm{rd}} = 1.2\,\mathrm{m}$ and $\eta = 0.5$

result considers a static AWGN channel for simplicity. For fading channels, channel estimation can be performed for each transmission [20] and the estimated channel information can then be used at the source node for rate adaptation.

5.5 Channel Estimation in Energy Harvesting Relaying

5.5.1 Introduction

Channel estimation is an important part of wireless relaying, as the destination needs the channel gains for signal demodulation and the relay may also need the channel gains for variable-gain amplification. There are a few existing works on channel estimation for relaying. For example, reference [21] discussed several linear minimum mean squared error (LMMSE) estimators for the cascaded channel coefficient as the product of the channel coefficient in the source-to-relay link and that in the relay-to-destination. Reference [22] proposed a new least squares (LS) estimator and reference [23] proposed a minimum mean squared error (MMSE) estimator, for the cascaded channel coefficient. References [24] and [25] proposed pilot-based moment-based (MB) estimators and maximum likelihood (ML) methods for the individual channel powers.

The previous sections analysed and proposed energy harvesting relaying schemes. In these schemes, the energy is mainly harvested for data transmission or data symbol forwarding in the relaying phase. Similar to data transmission, in pilot-based channel estimation, pilot symbols need to be transmitted or forwarded by the relay. Without energy harvesting, this transmission will bring a huge burden to the relay in terms of energy consumption and thus, will also discourage idle nodes from participating in relaying. Thus, it is important to adopt energy harvesting in the channel estimation of wireless relaying.

In this section, new pilot-based channel estimators for AF relaying are proposed. The pilots are sent using energy harvested from the source. Channel estimation is performed only using these pilots multiplexed in the time domain with the data symbols for single-carrier systems. Both TS and PS are considered. We propose several new estimation schemes using the approximate ML method. In Schemes 1 and 2, the relay harvests energy from pilots sent by the source and then uses this energy to forward pilots from the source as well as transmit its own pilots to the destination. In Schemes 3 and 4, the relay harvests energy from pilots sent by the source and also uses these pilots to estimate the source-to-relay link. Then, the harvested energy is used to transmit its own pilot to the destination to estimate the relay-to-destination link. Again, consider a three-node system without direct link. Assume that a total of K pilots are used in all schemes for energy harvesting and channel estimation. Each pilot occupies a time duration of T_p.

5.5.2 Scheme One

In Scheme 1, the relay harvests energy from the source using TS and then uses the harvested energy to forward pilots from the source as well as transmit its own pilots to the destination.

First, the source sends I pilots to the relay for energy harvesting. The received signal at the relay is given by

$$y_i^{(r-\mathrm{eh})} = \sqrt{P_s}h + n_i^{(r-\mathrm{eh})} \tag{5.27}$$

where $i = 1, 2, \ldots, I$, $n_i^{(r-\mathrm{eh})}$ is the AWGN with mean zero and variance $2\sigma_r^2$, and other symbols are defined as before. All the noise in this paper is assumed circularly symmetric. Using (5.27), the harvested energy is $E_h = \eta P_s |h|^2 I T_p$.

Second, the source sends another J_1 pilots to the relay, which will be forwarded to the destination for channel estimation. The received signal at the destination is

$$y_{j_1}^{(d-s)} = \sqrt{P_r} g a y_{j_1}^{(r-\mathrm{ce})} + n_{j_1}^{(d-s)}, \tag{5.28}$$

where $y_{j_1}^{(r-\mathrm{ce})} = \sqrt{P_s}h + n_{j_1}^{(r-\mathrm{ce})}$ is the forwarded pilot symbol, $j_1 = 1, 2, \ldots, J_1$, $n_{j_1}^{(r-\mathrm{ce})}$ is the AWGN at the relay with mean zero and variance $2\sigma_r^2$, and $n_{j_1}^{(d-s)}$ is the

AWGN at the destination with mean zero and variance $2\sigma_d^2$. In Scheme 1, since the relay does not perform channel estimation, fixed-gain relaying can be used such that one can set a as a constant for simplicity [15, 17].

Finally, in addition to forwarding J_1 pilots from the source, the relay also uses the harvested energy to transmit J_2 pilots of its own to the destination, giving

$$y_{j_2}^{(d-r)} = \sqrt{P_r} g + n_{j_2}^{(d-r)} \tag{5.29}$$

where $j_2 = 1, 2, \ldots, J_2$, $n_{j_2}^{(d-r)}$ is the AWGN at the destination during this transmission and is again complex Gaussian with mean zero and variance $2\sigma_d^2$. Using the harvested energy, since the relay has to forward J_1 pilots from the source and transmit J_2 pilots of its own, the transmission power of the relay can be written as $P_r = \frac{E_h}{JT_p} = \eta P_s |h|^2 \frac{I}{J}$, where $J = J_1 + J_2$.

The ML estimators can be derived as follows. Denote $G_y = \sqrt{\eta \frac{I}{J} P_s} |h| g$. Using the ML method, one log-likelihood function can be derived as $llf_1 = -J_2 \ln(2\pi\sigma_d^2) - \frac{1}{2\sigma_d^2} \sum_{j_2=1}^{J_2} |y_{d-r}^{(j_2)} - G_y|^2$. Thus, by differentiating llf_1 with respect to G_y, setting the derivative to zero and solving the equation for G_y, the ML estimate of G_y can be derived as

$$\hat{G}_y = \frac{1}{J_2} \sum_{j_2=1}^{J_2} y_{d-r}^{(j_2)} = \sqrt{\eta \frac{I}{J} P_s} |\hat{h}| \hat{g}. \tag{5.30}$$

Also, denote $H_y = \sqrt{P_s} h$. Using the ML method, another log-likelihood function can be derived as $llf_2 = -J_1 \ln(2\pi(1 + |G_y|^2 a^2)\sigma_d^2) - \frac{1}{2(1+|G_y|^2 a^2)\sigma_d^2} \sum_{j_1=1}^{J_1} |y_{d-s}^{(j_1)} - G_y H_y a|^2$. By differentiating llf_2 with respect to H_y, setting the derivative to zero and solving the equation for H_y, the ML estimate of H_y can be derived as

$$\hat{H}_y = \frac{1}{J_1 \hat{G}_y a} \sum_{j_1=1}^{J_1} y_{d-s}^{(j_1)} = \sqrt{P_s} \hat{h}. \tag{5.31}$$

The invariance principle of ML estimation states that a function of ML estimate is the ML estimate of that function [26]. Using this principle, the ML estimates of g and h can be derived by solving (5.30) and (5.31) for $\hat{g}$ and $\hat{h}$, which gives

$$\hat{g}_1 = \frac{\frac{1}{J_2} \sum_{j_2=1}^{J_2} y_{d-r}^{(j_2)} |\frac{1}{J_2} \sum_{j_2=1}^{J_2} y_{d-r}^{(j_2)}|}{\frac{1}{a} \sqrt{\eta \frac{I}{J}} |\frac{1}{J_1} \sum_{j_1=1}^{J_1} y_{d-s}^{(j_1)}|} \tag{5.32}$$

$$\hat{h}_1 = \frac{1}{\sqrt{P_s} a} \frac{\frac{1}{J_1} \sum_{j_1=1}^{J_1} y_{d-s}^{(j_1)}}{\frac{1}{J_2} \sum_{j_2=1}^{J_2} y_{d-r}^{(j_2)}} \tag{5.33}$$

These ML estimators are approximate estimators because the exact ML estimators should be obtained by multiplying llf_1 with llf_2 and using the joint function for estimation. However, this renders complicated nonlinear functions of g and h and hence, it is not used here. Since both $y_{d-s}^{(j_1)}$ and $y_{d-r}^{(j_2)}$ are samples received at the destination, the relay does not perform channel estimation. This reduces the complexity at the relay.

5.5.3 Scheme 2

Scheme 2 is similar to Scheme 1, except that the energy is harvested using PS. First, the source sends K_1 pilots to the relay. Part of the received signal at the relay is used for channel estimation as $z_{k_1}^{(r-\text{ce})} = \sqrt{(1-\rho)P_s}h + n_{k_1}^{(r-\text{ce})}$, which is forwarded to the destination to give

$$z_{k_1}^{(d-s)} = \sqrt{P_r}gaz_{k_1}^{(r-\text{ce})} + n_{k_1}^{(d-s)} \tag{5.34}$$

where $k_1 = 1, 2, \ldots, K_1$ index the pilots from the source, ρ is the PS factor, $n_{k_1}^{(r-\text{ce})}$ and $n_{k_1}^{(d-s)}$ are the AWGN with means zero and variances $2\sigma_r^2$ and $2\sigma_d^2$, respectively. The other part of the received power at the relay is harvested as $E_h = \eta\rho P_s|h|^2 K_1 T_p$.

Second, the relay also transmits K_2 its own pilots to the destination such that the received signal at the destination is

$$z_{k_2}^{(d-r)} = \sqrt{P_r}g + n_{k_2}^{(d-r)} \tag{5.35}$$

where $k_2 = 1, 2, \ldots, K_2$ and $n_{k_2}^{(d-r)}$ is the AWGN with mean zero and variance $2\sigma_d^2$. Since the relay forwards K_1 pilots from the source and transmits K_2 pilots of its own, a total of $K = K_1 + K_2$ pilots will be sent to the destination such that $P_r = \frac{E_h}{KT_p} = \eta\rho P_s|h|^2\frac{K_1}{K}$.

The ML estimators are derived as follows. Denote $G_z = \sqrt{\eta\rho P_s\frac{K_1}{K}}|h|g$ and $H_z = \sqrt{(1-\rho)P_s}h$. Similar to before, using the samples and the ML method, the ML estimate of G_z can be derived as $\hat{G}_z = \frac{1}{K_2}\sum_{k_2=1}^{K_2} z_{d-r}^{(k_2)} = \sqrt{\eta\rho P_s\frac{K_1}{K}}|\hat{h}|\hat{g}$ and using the samples and the ML method, the ML estimate of H_z can be derived as $\hat{H}_z = \frac{1}{K_1\hat{G}_z a}\sum_{k_1=1}^{K_1} z_{d-s}^{(k_1)} = \sqrt{(1-\rho)P_s}\hat{h}$. Using the invariance principle, the ML estimators for g and h can be obtained as

$$\hat{g}_2 = \frac{a\sqrt{1-\rho}}{\sqrt{\eta\rho\frac{K_1}{K}}}\frac{\frac{1}{K_2}\sum_{k_2=1}^{K_2} z_{d-r}^{(k_2)}|\frac{1}{K_2}\sum_{k_2=1}^{K_2} z_{d-r}^{(k_2)}|}{|\frac{1}{K_1}\sum_{k_1=1}^{K_1} z_{d-s}^{(k_1)}|} \tag{5.36}$$

and

$$\hat{h}_2 = \frac{1}{\sqrt{(1-\rho)P_s a}} \frac{\frac{1}{K_1}\sum_{k_1=1}^{K_1} z_{d-s}^{(k_1)}}{\frac{1}{K_2}\sum_{k_2=1}^{K_2} z_{d-r}^{(k_2)}} \tag{5.37}$$

respectively. Again, only the destination needs to perform channel estimation to reduce complexity at the relay.

5.5.4 Scheme 3

In Scheme 3, first, the source sends J_1 pilots to the relay such that the received signal at the relay is

$$u_{j_1}^{(r-\mathrm{ce})} = \sqrt{P_s}h + n_{j_1}^{(r-\mathrm{ce})} \tag{5.38}$$

where $j_1 = 1, 2, \ldots, J_1$ and $n_{j_1}^{(r-\mathrm{ce})}$ is the AWGN with mean zero and variance $2\sigma_r^2$. Second, the source sends I pilots to the relay for energy harvesting. The harvested energy is $E_h = \eta P_s |h|^2 I T_p$. Finally, the relay uses the harvested energy to transmit J_2 pilots of its own to the destination. The transmission power of the relay is $P_r = \frac{E_h}{J_2 T_p} = \eta P_s |h|^2 \frac{I}{J_2}$ and the received signal at the destination is

$$u_{j_2}^{(d-r)} = \sqrt{\eta P_s \frac{I}{J_2}}|h|g + n_{j_2}^{(d-r)} \tag{5.39}$$

where $j_2 = 1, 2, \ldots, J_2$. In the above, $n_{j_1}^{(r-\mathrm{ce})}$ and $n_{j_2}^{(d-r)}$ are again circularly symmetric AWGN with means zero and variances $2\sigma_r^2$ and $2\sigma_d^2$, respectively.

The ML estimators can also be derived. Using (5.38), since there is only one unknown parameter in the log-likelihood function, the ML estimator for h can be easily derived. Also, denote $G_u = \sqrt{\eta P_s \frac{I}{J_2}}|h|g$. Using (5.39), the ML estimate of G_u can be derived as $\hat{G}_u = \frac{1}{J_2}\sum_{j_2=1}^{J_2} u_{d-r}^{(j_2)} = \sqrt{\eta P_s \frac{I}{J_2}}|\hat{h}|\hat{g}$. Then, using the invariance principle, the ML estimators are

$$\hat{g}_3 = \frac{\frac{1}{J_2}\sum_{j_2=1}^{J_2} u_{d-r}^{(j_2)}}{\sqrt{\eta \frac{I}{J_2}}|\frac{1}{J_1}\sum_{j_1=1}^{J_1} u_{r-\mathrm{ce}}^{(j_1)}|} \tag{5.40}$$

and

$$\hat{h}_3 = \frac{1}{\sqrt{P_s}} \frac{1}{J_1} \sum_{j_1=1}^{J_1} u_{r-\mathrm{ce}}^{(j_1)}. \tag{5.41}$$

Note that, in this scheme, the relay estimates h and its estimate has to be sent to the destination via control channels for the estimation of g at the destination. Thus, this scheme is more complicated than Schemes 1 and 2.

5.5.5 Scheme 4

Scheme 4 is similar to Scheme 3, except that the relay uses PS to harvest energy. First, the source sends K_1 pilots to the relay, part of which is received for channel estimation as

$$v_{k_1}^{(r-\mathrm{ce})} = \sqrt{(1-\rho)P_s}h + n_{k_1}^{(r-\mathrm{ce})} \tag{5.42}$$

for $k_1 = 1, 2, \ldots, K_1$ and part of which is harvested with $E_h = \eta\rho P_s|h|^2 K_1 T_p$. Second, the relay uses the harvested energy to transmit K_2 pilots of its own such that the received signal at the destination is

$$v_{k_2}^{(d-r)} = \sqrt{\eta\rho P_s \frac{K_1}{K_2}}|h|g + n_{k_2}^{(d-r)} \tag{5.43}$$

for $k_2 = 1, 2, \ldots, K_2$. Note that $n_{k_1}^{(r-\mathrm{ce})}$ and $n_{k_2}^{(d-r)}$ are also circularly symmetric AWGN with means zero and variances $2\sigma_r^2$ and $2\sigma_d^2$, respectively.

Using (5.42) and (5.43), the ML estimators for g and h can be derived in a similar way as

$$\hat{g}_4 = \frac{\frac{1}{K_2}\sum_{k_2=1}^{K_2} v_{d-r}^{(k_2)}}{\sqrt{\eta\frac{K_1}{K_2}\frac{\rho}{1-\rho}}|\frac{1}{K_1}\sum_{k_1=1}^{K_1} v_{r-\mathrm{ce}}^{(k_1)}|} \tag{5.44}$$

and

$$\hat{h}_4 = \frac{1}{\sqrt{(1-\rho)P_s}}\frac{1}{K_1}\sum_{k_1=1}^{K_1} v_{r-\mathrm{ce}}^{(k_1)}. \tag{5.45}$$

5.5.6 Numerical Results

In this section, the new estimators will be examined. We set $\eta = 0.5$, $P_s = 1$, $K = 100$ and $2\sigma_r^2 = 2\sigma_d^2 = 2$. Define $\gamma_g = \frac{|g|^2}{2\sigma_d^2}$, $\gamma_h = \frac{|h|^2}{2\sigma_r^2}$. The values of g and h will change with γ_g and γ_h and their real and imaginary parts equal to each other. The normalized mean squared error (MSE) is defined as $\frac{1}{R|g|^2}\sum_{r=1}^{R}|\hat{g}_r - g|^2$,

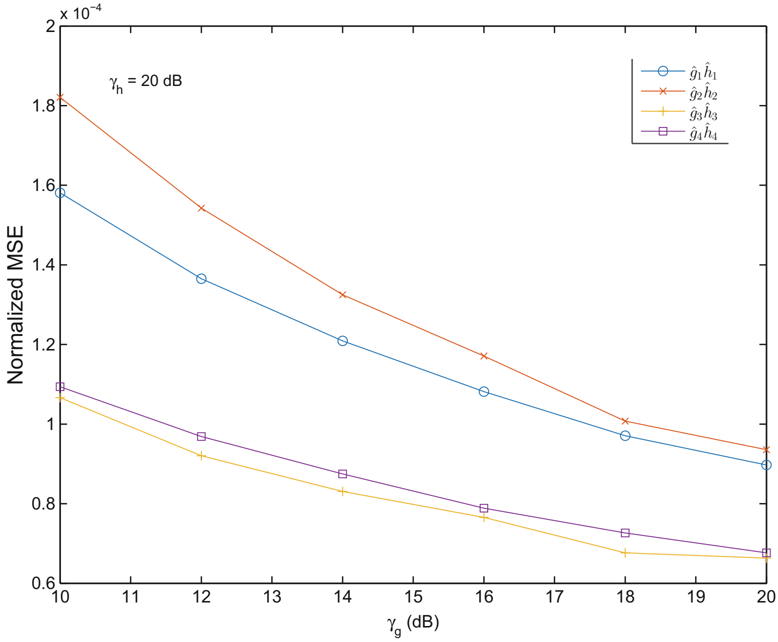

Fig. 5.19 Minimum normalized MSE of $\hat{g}\hat{h}$ vs. γ_g for different schemes

$\frac{1}{R|h|^2}\sum_{r=1}^{R}|\hat{h}_r - h|^2$, $\frac{1}{R|gh|^2}\sum_{r=1}^{R}|\hat{g}_r\hat{h}_r - gh|^2$ for $\hat{g}$, $\hat{h}$ and $\hat{g}\hat{h}$, respectively, where R is the total number of simulation runs and $\hat{g}_r$ and $\hat{h}_r$ are the channel estimates in the r-th run.

Figures 5.19 and 5.20 compare the estimators in terms of their minimum normalized MSEs of $\hat{g}\hat{h}$ achieved by performing exhaustive searches over the relevant parameters. One sees that Schemes 3 and 4 have the best performances, and Schemes 1 and 2 have the worst performance. Also, TS is better than PS in most cases.

5.5.7 Conclusion

New pilot-based ML estimators for AF relaying have been proposed by using harvested energy to transmit or forward pilots. Numerical results have been presented to show their performances. It is concluded that the two schemes that perform channel estimation only at the destination are the simplest but have the worst performances in terms of MSE. Note that the proposed estimators use pilots only, similar to some previous works. No data symbols are available for energy harvesting in the estimation. One could extend this scheme to blind or semi-blind estimation, where energy can also be harvested from data symbols.

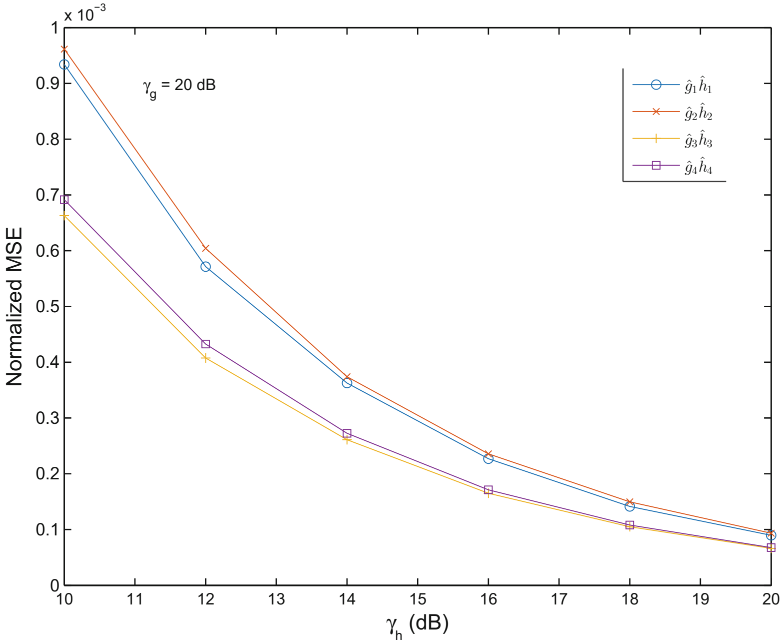

Fig. 5.20 Minimum normalized MSE of $\hat{g}\hat{h}$ vs. γ_h for different schemes

5.6 Summary

In this chapter, the performance of wireless powered relaying has been analysed in the absence or presence of co-channel interference. The analysis has shown the benefit of using energy harvesting or wireless power to reduce the energy consumption at the relay. Moreover, new energy harvesting relaying protocols have been designed to improve the system energy efficiency further. As an important part of wireless relaying, channel estimation in the context of energy harvesting has also been studied and several new channel estimators have been proposed. Owing to the many benefits offered by wireless power, energy harvesting relaying has seen wider use in emerging applications, such as massive multiple-input-multiple-output [27]. Also, in addition to the schemes discussed in this chapter, there are quite a few works focusing on the optimal use of the harvested energy in the relaying process [28, 29]. Finally, the above results only consider the case when the direct link between source and destination does not exist. It may be possible to extend these results to the case when the direct link exists. For example, in Sect. 5.2.2, assuming that the direct link is independent of the relaying link, the overall BER may be modified by combining (3) with the BER of the direct link, depending on the decision fusion rules. Also, in Sect. 5.2.3, assuming selection combining, the throughput of the relaying link in (5) can be combined with the throughput of the direct link. However, for Sect. 5.3, this extension may be difficult.

References

1. M. Peng, Y. Liu, D. Wei, W. Wang, H.-H. Chen, Hierarchical cooperative relay based heterogeneous networks. IEEE Wirel. Commun. **18**, 48–56 (2011)
2. B. Zhou, H. Hu, S.-Q. Huang, H.-H. Chen, Intracluster device-to-device relay algorithm with optimal resource allocation. IEEE Trans. Veh. Technol. **62**, 2315–2326 (2013)
3. J.N. Laneman, G.W. Wornell, Energy-efficient antenna sharing and relaying for wireless networks, in *Proceedings of 2000 IEEE Wireless Communication Networking Conference (WCNC)*, Chicago, vol. 1, March (2000), pp. 7–12
4. J.N. Laneman, D.N.C. Tse, G.W. Wornell, Cooperative diversity in wireless networks: efficient protocols and outage behaviors. IEEE Trans. Inf. Theory **50**, 3062–3080 (2004)
5. R. Zhang, C.K. Ho, MIMO broadcasting for simultaneous wireless information and power transfer. IEEE Trans. Wirel. Commun. **12**(5), 1989–2001 (2013)
6. Z. Ding, I. Krikidis, B. Sharif, H.V. Poor, Wireless information and power transfer in cooperative networks with spatially random relays. IEEE Trans. Wirel. Commun. **13**, 4440–4453 (2014)
7. A.A. Nasir, X. Zhou, S. Durrani, R.A. Kennedy, Throughput and ergodic capacity of wireless energy harvesting based DF relaying network, in *Proceedings of IEEE ICC 2014*, pp. 4066–4071, Sydney, June (2014)
8. Y. Gu, S. Aissa, Interference aided energy harvesting in decode-and-forward relaying systems, in *Proceedings of IEEE ICC 2014*, pp. 5378–5382, Sydney, June (2014)
9. H.A. Suraweera, G. Zheng, I. Krikidis, Z. Zhang, Wireless information and power transfer with full duplex relaying. IEEE Trans. Commun. **62**, 3447–3461 (2014)
10. M. Mohammadi, B.K. Chalise, H.A. Suraweera, C. Zhong, G. Zheng, I. Krikidis, Throughput analysis and optimization of wireless-powered multiple antenna full-duplex relay systems. IEEE Trans. Commun. **64**, 1769–1785 (2016)
11. I.S. Gradshteyn, I.M Ryzhik, *Table of Integrals, Series and Products*, 7th edn. (Academic, London, 2007)
12. A.A. Nasir, X. Zhou, S. Durrani, R.A. Kennedy, Relaying protocols for wireless energy harvesting and information processing. IEEE Trans. Wirel. Commun. **12**, 3622–3636 (2013)
13. I. Krikidis, G. Zhang, B. Ottersten, Harvest-use cooperative networks with half/full-duplex relaying, in *Proceedings of WCNC'13*, pp. 4256–4260 (2013)
14. Z. Ding, S.M. Perlaza, I. Esnaola, H.V. Poor, Power allocation strategies in energy harvesting wireless cooperative networks. IEEE Trans. Wirel. Commun. **13**, 846–860 (2014)
15. M.O. Hasna, M.-S. Alouini, A performance study of dual-hop transmissions with fixed gain relays. IEEE Trans. Wirel. Commun. **3**, 1963–1968 (2004)
16. G.K. Karagiannidis, Performance bounds of multihop wireless communications with blind relays over generalized fading channels. IEEE Trans. Wirel. Commun. **5**, 498–503 (2006)
17. M. Di Renzo, F. Graziosi, F. Santucci, A comprehensive framework for performance analysis of dual-hop cooperative wireless systems with fixed-gain relays over generalized fading channels. IEEE Trans. Wirel. Commun. **8**, 5060–5074 (2009)
18. Y. Chen, Energy-harvesting AF relaying in the presence of interference and Nakagami-m fading. IEEE Trans. Wirel. Commun. **15**, 1008–1017 (2016)
19. H. Meyr, M. Mseneclaey, S.A. Fechtel, *Digital Communication Receivers, Synchronization, Channel Estimation, and Signal Processing* (Wiley, New York, 1998)
20. F.H. Khan, Y. Chen, M.-S. Alouini, Novel receivers for AF relaying with distributed STBC using cascaded and disintegrated channel estimation. IEEE Trans. Wirel. Commun. **11**, 1370–1379 (2012)
21. C.S. Patel, G.L. Stuber, Channel estimation for amplify and forward relay based cooperation diversity systems. IEEE Trans. Wirel. Commun. **6**, 2348–2356 (2007)
22. P. Lioliou, M. Viberg, M. Coldrey, Efficient channel estimation techniques for amplify and forward relaying systems. IEEE Trans. Commun. **60**, 3150–3155 (2012)

23. F. Gao, T. Cui, A. Nallanathan, On channel estimation and optimal training design for amplify and forward relay networks. IEEE Trans. Wirel. Commun. **7**, 1907–1916 (2008)
24. H. Yomo, E. de Carvalho, A CSI estimation method for wireless relay networks. IEEE Commun. Lett. **11**, 480–482 (2007)
25. N. Aerts, M. Moeneclaey, Pilot-based ML estimation in amplify-and-forward cooperative networks, in *Proceedings of IEEE WCNC 2012*, Shanghai (2012), pp. 1044–1048
26. S. Kay, *Fundamentals of Statistical Signal Processing: Estimation Theory* (Prentice Hall, London, 1993)
27. G. Amarasuriya, E.G. Larsson, H.V. Poor, Wireless information and power transfer in multiway massive MIMO relay networks. IEEE Trans. Wirel. Commun. **15**, 3837–3855 (2016)
28. A. Rajaram, D.N.K. Jayakody, V. Skachek, Store-then-cooperate: energy harvesting scheme in cooperative relay networks, in *Proceedings of 13th International Symposium on Wireless Communication Systems (ISWCS'16)*, Poznan, Sept 2016
29. H. Chen, Y. Li, J.L. Rebelatto, B.F. Uchoa-Filho, B. Vucetic, Harvest-then-cooperate: wireless-powered cooperative communications. IEEE Trans. Signal Process. **63**(7), 1700–1711 (2015)